Pentabasic Thermoelectricity System Prepared by Powder Metallurgy Method and the Performance Thermoelectric Generator Modules

Ye Guo, Jiangduo Wang, Yuanfa Deng, Chulan Lu, Yiping Luo and Bin Lin

Abstract With the technological development and awareness of energy conservation and environmental protection, how to take advantage of waste heat has been concerned global. However, effective methods to recycle low temperature waste heat which is lower than 200 °C are still lacked. A kind of pentabasic thermoelectricity system which is prepared by smelting and powder metallurgy method is described in this paper. Thermoelectric generator (TEG) modules with different area and height ratio (A/H) p-n couples are assembled. At temperature gradient 100 K, the TEG module can obtain the biggest load power 2.39 W corresponding the module with A/H = 5.5 and load resistance 1.5 Ω.

Keywords Low temperature waste heat · Thermoelectric generator modules Area and height ratio · Load power

Introduction

Only no more than 40% energy is make good use by current energy conversion technologies and the other energy dissipate by style of waste heat primarily [1]. However, recycling low temperature waste heat distributing from 50 to 200 °C that have low thermal flux density is more challenging than high temperature waste heat in industry [2, 3].

Thermoelectric material and related technology, as a low-carbon energy conversion technique, can take advantage of automobile exhaust gas or industrial waste heat and then convert it to direct current [4–7]. The performance of thermoelectric material is related to its intrinsic properties which can be described by the

Y. Guo · J. Wang · Y. Deng · C. Lu · Y. Luo (✉) · B. Lin (✉)
Guangdong Leizig Thermoelectric Technologies Co., Ltd.,
Guangzhou 510470, Guangdong, China
e-mail: yale_guo@leizig.com

B. Lin
e-mail: tu_luo@leizig.com

Y. Han (ed.), *Advances in Energy and Environmental Materials*,
Springer Proceedings in Energy, https://doi.org/10.1007/978-981-13-0158-2_4

dimensionless figure of merit ZT = $\alpha^2\sigma/\kappa$, where α is the Seebeck coefficient, σ is the electrical conductivity, κ is the thermal conductivity, and T is the absolute temperature. This three parameters α, σ and κ are relate to each other [8–10].

In practical application, whether they are used for cool or generator, the modules were assembled in series by many p-n couples. Nevertheless, to acquire high performance TEG modules, both p-type and n-type require not only excellent ZT value but also good compatibility between them. The good compatibility mean the number and curve of Seebeck coefficient, electrical conductivity and ZT value are approximate and have similar varying tendency in their working temperature interval [11–18]. And similar electrical conductivity is the most important factor.

In this work, we introduce a pentabasic thermoelectricity system which is consisted of five elements Bi, Sb, S, Te and Se. P-type and n-type thermoelectric material can be obtained by adjusting the ratios of this five elements. It can be more easily to acquire good compatibility between p-type and n-type materials they have similar chemical constitution. TEG modules with different height p-n couples are assembled. The power output of open-circuit voltage, short-circuit current and the resistive load power of those TEG module were measured and discussed.

Experimental

Sample Preparation. P-type and n-type samples were synthesized by direct solid state reaction. High purity starting elements, Bi (99.999%), Sb (99.999%), S (99.999%), Te (99.999%) and Se (99.999%) were weighted out in stoichiometric ratios and added into quartz ampoules which were evacuated to <1 Pa. Then the evacuated ampoules were placed into a resistance melting furnace and heated with 2 °C/min to 650 °C and held at that temperature for 48 h. And then they were cooled to room temperature naturally. The resulting alloys were broken to powder and put into a stainless steel pots and ball milled for 60 min in full-directional planetary ball mill. Those ball-milled powders were cold pressed into a column with the pressure 900 Mpa and annealed under vacuum for 6 h at 400 °C. Then they were cooled to room temperature naturally with 1 °C/min to acquire final product.
Module Fabrication. The TEG modules with dimensions of 40 * 45 mm and different p-n couple height were fabricated by automatic die bonder. 127 pairs of p-n couples were assembled electrically in series with aluminium oxide ceramic substrates as electrical insulator foundation. The structure graph of our TEG modules is shown in Fig. 1. Nickel was chosen on TE materials as the diffusion barrier to inhibit element diffusions between the TE materials and the solder and copper was used as the electrode. The cross section area of all p or n leg is 1.7 * 1.7 mm^2. The height of p and n leg is 0.42, 0.52, 0.82, 0.92 and 1.00 mm. It means that the area and height ratio (A/H) of p-n legs is 6.80, 5.50, 4.62, 3.50, 3.12 and 2.89 respectively.

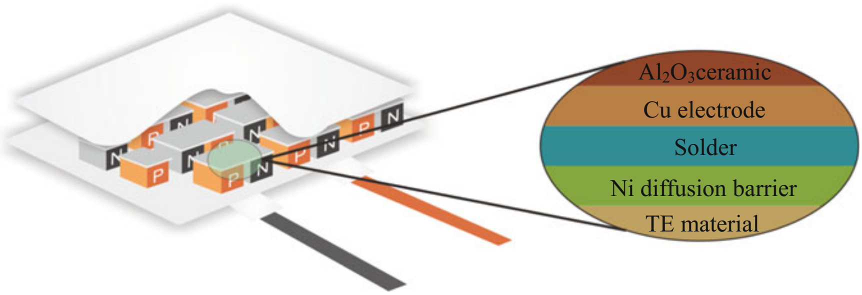

Fig. 1 Structure graph of TEG module

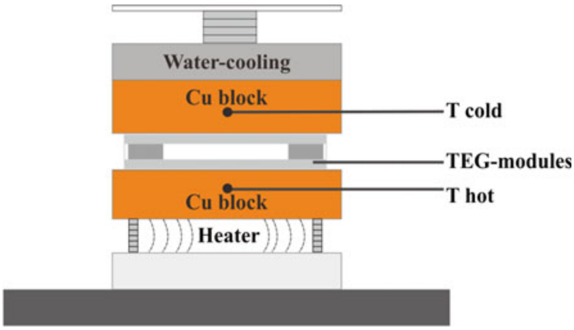

Fig. 2 Structure graph of homebuilt testing device

Testing. The Seebeck coefficient and electrical conductivity and at 298–473 K were measured using Linseis LSR-3/1100 under vacuum environment. Thermal conductivity at 298–473 K was calculated by multiplied the thermal diffusivity, heat capacity and sample density. The thermal diffusivity was measured at argon atmosphere using a laser flash method (FL4010, TA Co. Ltd.). The heat capacity was measured using DSC 200 F3 (Netzsch Co. Ltd.). The density was measured by Archimedes method. The power output of open-circuit voltage, short-circuit current, load voltage, load current and the resistive load power of the TEG module were measured by our homebuilt testing device (Fig. 2). Tow copper blocks were used to connect heater that can heat to 300 °C and circulating water cooling. The TEG module was placed between those two copper blocks. And load resistance is provided by DC Electronic Load (ITECH, IT8511+) which can change resistance easily and display load resistance, load current, load voltage and load power. Open-circuit voltage and short-circuit current were tested with temperature gradient from 10 to 130 K and resistive load characteristics were measured at temperature gradient 100 K.

Results and Discussion

Electric Properties of Materials. Figure 3a displays the temperature dependence of Seebeck coefficient p-type and n-type materials. The curve of those two materials have similar varying tendency in the temperature interval from 298 to 473 K (25–200 °C). Figure 3b shows the temperature dependence of electric conductivity of p-type and n-type samples from 298 to 473 K. Original electric conductivity of those tow material is about 50,000 S/m at 298 K and decline synchronously with temperature increasing. The temperature dependence of the thermal conductivity is shown in Fig. 3c. Thermal conductivity of p-type sample is lower than 0.75 $Wm^{-1}K^{-1}$ and n-type sample is lower than 0.90 $Wm^{-1}K^{-1}$. As shown in Fig. 4d, figure of merit ZT was calculated. The p-type sample has a good performance in ZT value which is 1.24 at 348 K and has an average value about 1. Although perfect compatibility electrical conductivity is acquired between p-type and n-type materials, ZT value of n-type materials isn't an ideal level obviously.

Electric Properties of TEG Modules. Modules resistance with A/H 6.80, 5.50, 4.62, 3.50, 3.12 and 2.89 are 0.72, 0.84, 0.91, 1.43, 1.59 and 1.42 Ω. The abnormal

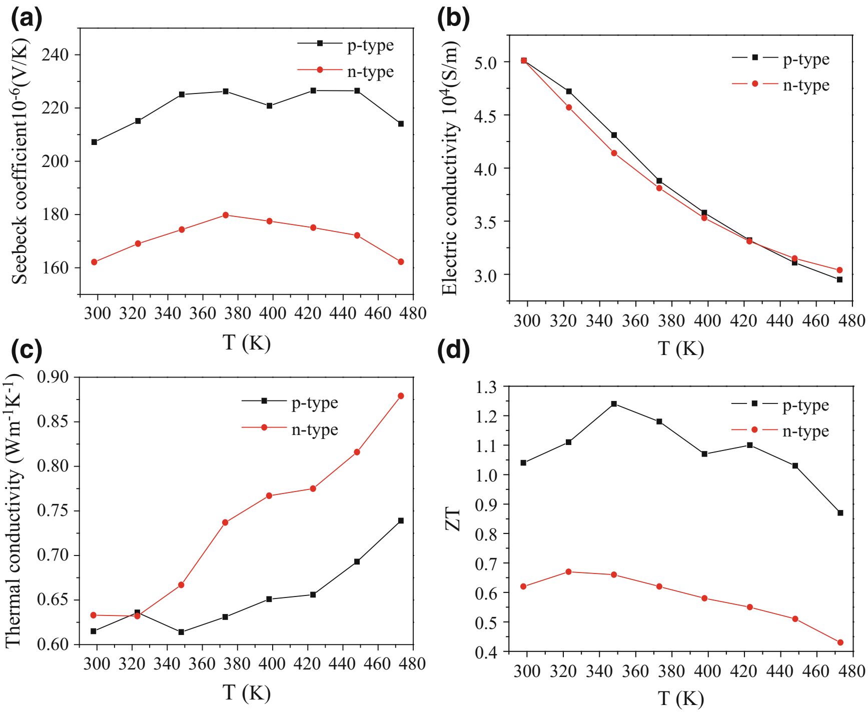

Fig. 3 Temperature dependence of **a** the Seebeck coefficient, **b** electrical conductivity, **c** thermal conductivity and **d** figure of merit ZT for p-type and n-type samples from 298 to 473 K

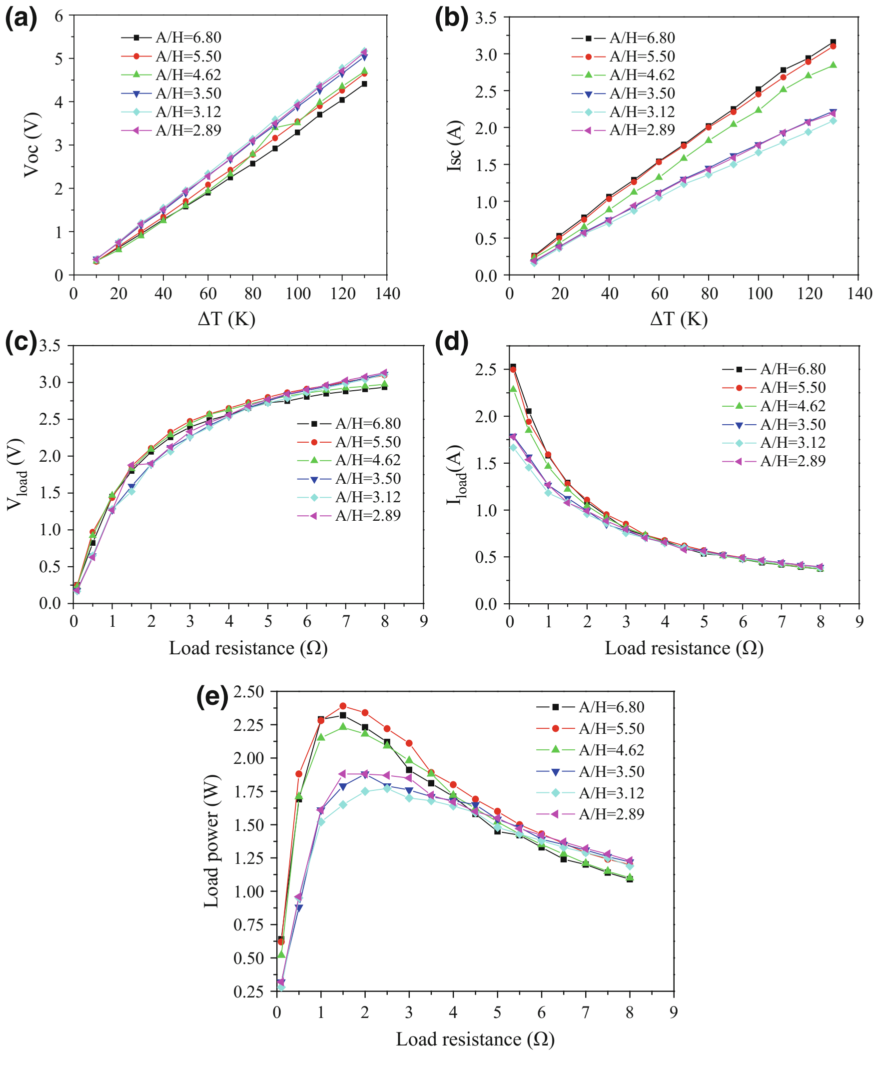

Fig. 4 Electric properties of TEG modules **a** temperature dependence of open-circuit voltage, **b** temperature dependence of short-circuit current, **c** load current temperature gradient 100 K, **d** load voltage temperature gradient 100 K and **e** load power temperature gradient 100 K

resistance for A/H = 2.89 is on account of the samples were experienced tow times cold pressing and sintering process. Figure 4a, b displays the open-circuit voltage and short-circuit current of TEG modules with a series of A/H respectively. Figure 4c–e shows load current, load voltage and load power with the load resistance range from 0.1 to 8 Ω. Electric properties of TEG modules, especially the current and the load power, increase with the A/H changing from 2.89 to 6.80. And the biggest load power is 2.39 W corresponding the module with A/H = 5.5 and load resistance 1.5 Ω. Heat flux Q was obtained based on the one-dimensional Fourier's law [19, 20]: $Q = \kappa * A * \Delta T/L$ where κ and A are the thermal conductivity and the cross-sectional area, respectively. ΔT is the temperature difference measured by the thermocouples embedded in the two Cu block and L is the vertical distance between the two thermocouples. The cross section area of all p or n leg is $1.7 * 1.7\ mm^2$. It is obvious that the higher A/H can lead to lower L and higher Q. Although higher A/H and Q is good for achieving bigger output power, in actual application, heat dissipation potential on cold side must be considered.

Conclusion

In summary, p-type and n-type material with perfect compatibility on electrical conductivity were acquired by this method easily to realize mass production. The optimal ZT value for p-type material is 1.24 at 348 K. Electric properties of TEG modules increase with the A/H adding from 2.89 to 6.80 and the biggest load power is 2.39 W corresponding the module with A/H = 5.5 and load resistance 1.5 Ω at temperature gradient 100 K. However, in practical application, heat dissipation capacity on cold side must be considered to acquire ideal temperature gradient and output power.

Acknowledgements This work was supported by the Guangdong Leizig Thermoelectric Technologies Co., Ltd.

References

1. M. Zebarjadi, K. Esfarjani, M.S. Dresselhaus, Z.F. Ren, G. Chen, Perspectives on thermoelectrics: from fundamentals to device applications. Energy Environ. Sci. **5**, 5147 (2012)
2. D. Wang, X. Ling, H. Peng, L. Liu, L. Tao, Efficiency and optimal performance evaluation of organic Rankine cycle for low grade waste heat power generation. Energy **50**, 343 (2013)
3. Z. Wang, N. Zhou, J. Guo, X. Wang, Fluid selection and parametric optimization of organic Rankine cycle using low temperature waste heat. Energy **40**, 107–115 (2012)
4. J.W. Fergus, Oxide materials for high temperature thermoelectric energy conversion. J. Eur. Ceram. Soc. **32**, 525–540 (2012)
5. G.J. Snyder, E.S. Toberer, Complex thermoelectric materials. Nat. Mater. **7**, 105 (2008)
6. A.J. Minnich, M.S. Dresselhaus, Z.F. Ren, G. Chen, Bulk nanostructured thermoelectric materials: current research and future prospects. Energy Environ. Sci. **2**, 466–479 (2009)
7. M. Barati, S. Esfahani, T.A. Utigard, Energy recovery from high temperature slags. Energy **36**, 5440 (2011)
8. X.W. Wang, H. Lee, Y.C. Lan, G.H. Zhu, G. Joshi, D.Z. Wang, J.Yang, A.J. Muto, M.Y. Tang, J. Klatsky, S. Song, M.S. Dresselhaus, G. Chen, Z.F. Ren, Enhanced thermoelectric figure of merit in nanostructured n-type silicon germanium bulk alloy. Appl. Phys. Lett. **93**, 193121 (2008)

9. J.R. Sootsman, D.Y. Chung, M.G. Kanatzidis, New and old concepts in thermoelectric materials. Angew. Chem. Int. Edit. **48**, 8616–8639 (2009)
10. J.P. Heremans, V. Jovovic, E.S. Toberer, A. Saramat, K. Kurosaki, A. Charoenphakdee, S. Yamanaka, G.J. Snyder, Enhancement of thermoelectric efficiency in PbTe by distortion of the electronic density of states. Science **321**, 554–557 (2008)
11. Q.H. Zhang, X.Y. Huang, S.Q. Bai, X. Shi, C. Uher, L.D. Chen, Thermoelectric devices for power generation: recent progress and future challenges. Adv. Eng. Mater. **18**, 194–213 (2016)
12. D. Kraemer, J. Sui, K. McEnaney, H. Zhao, Q. Jie, Z.F. Renand, G. Chen, High thermoelectric conversion efficiency of MgAgSb-based material with hot-pressed contacts. Energy Environ. Sci. **8**, 1299–1308 (2015)
13. P.A. Zong, R. Hanus, M. Dylla, Y.S. Tang, J.C. Liao, Q.H. Zhang, G.J. Snyder, L.D. Chen, Skutterudite with graphene-modified grain-boundary complexion enhances zT enabling high-efficiency thermoelectric device. Energy Environ. Sci. **10**, 183–191 (2017)
14. Y.S. Park, T. Thompson, Y. Kim, J.R. Salvador, J.S. Sakamoto, Protective enamel coating for n- and p-type skutterudite thermoelectric materials. J. Mater. Sci. **50**, 1500–1512 (2015)
15. J.R. Salvador, J.Y. Cho, Z. Ye, J.E. Moczygemba, A.J. Thompson, J.W. Sharp, J.D. Koenig, R. Maloney, T. Thompson, J. Sakamoto, H. Wang, A.A. Wereszczak, Power-generation characteristics after vibration and thermal stresses of thermoelectric unicouples with $CoSb_3$/Ti/Mo(Cu) interfaces. Phys. Chem. Chem. Phys. **16**, 12510–12520 (2014)
16. H.S. Kim, W.S. Liu, Z.F. Ren, The bridge between the materials and devices of thermoelectric power generators. Energy Environ. Sci. **10**, 69–85 (2017)
17. T. Sakamoto, Y. Taguchi, T. Kutsuwa, K. Ichimi, S. Kasatani, M. Inada, Investigation of barrier-layer materials for Mg_2Si/Ni interfaces. J. Electron. Mater. **45**, 321–1327 (2016)
18. M. Gu, X.G. Xia, X.Y. Huang, S.Q. Bai, X.Y. Li, L.D. Chen, Study on the interfacial stability of p-type Ti/$Ce_yFe_xCo_{4-x}Sb_{12}$ thermoelectric joints at high temperature. J. Alloys Compd. **671**, 238–244 (2016)
19. F. Hao, P. Qiu, Y. Tang, S. Bai, High efficiency Bi_2Te_3-basedmaterials and devices for thermoelectric power generation between 100 and 300 °C. Energy Environ. Sci. **9**, 3120 (2016)
20. Q. Zhang, J. Liao, Y. Tang, M. Gu, C. Ming, P. Qiu, S. Bai, X. Shi, C. Uher, L. Chen, Realizing a thermoelectric conversion efficiency of 12% in bismuth telluride/skutterudite segmented modules through full-parameter optimization and energy-loss minimized integration. Energy Environ. Sci. **10**, 956–963 (2017)